Vertical sorting and the morphodynamics of bed form-dominated rivers: A sorting evolution model. 2. Application

Astrid Blom

Water Engineering & Management, Civil Engineering, University of Twente, Netherlands

Jan S. Ribberink

Water Engineering & Management, Civil Engineering, University of Twente, Netherlands

Gary Parker

Department of Civil and Environmental Engineering and Department of Geology, University of Illinois at Urbana-Champaign, Urbana, Illinois, USA

Abstract. A new sediment continuity model for conditions dominated by dunes, nonuniform sediment, and bed load transport is used to simulate two flume experiments. In the accompanying paper [*Blom et al.*, 2007], this sorting evolution model model is proposed and components of the morphodynamic model system have been discussed. In the present paper, we compare the predicted time evolution of the vertical sorting profile to the measured one for two flume experiments. Also, the predicted time evolution of the grain size distribution of the bed load transport has been compared to the measured one. The sorting evolution model shows reasonable results, although the formation of a coarse bed layer underneath the migrating bed forms is not well reproduced. It is therefore suggested to incorporate sorting mechanisms as partial transport and the winnowing of fines from the trough surface and subsurface in a future version of the model.

1. Introduction

Focussing on rivers dominated by nonuniform sediment, bed forms, and bed load transport, *Blom and Parker* [2004] adapt formulations for entrainment and deposition densities as required for the depth-continuous framework for sediment continuity developed by *Parker et al.* [2000]. Such a sediment continuity framework describes the interaction among grain size-selective sediment transport, vertical sorting and net aggradation of the river bed. While *Blom et al.* [2006] reduce the *Blom and Parker* [2004] sediment continuity framework to equilibrium or steady conditions, in an accompanying paper [*Blom et al.*, 2007], we derive a model that includes the effects of the time evolution of the sorting

profile on the morphodynamic evolution of the bed, i.e. the sorting evolution model. In the present paper we apply this new sediment continuity model to two flume experiments and compare the predicted time evolution of the sorting profile to measured data. For further information on the development of the sediment continuity model, we refer to the introduction in the accompanying paper [*Blom et al.*, 2007].

2. The flume experiments

The verification of the sorting evolution model is based on a comparison between the measured and computed sorting profiles for experiments B2 and A2 [*Blom et al.*, 2003]. The experiments were conducted in the Sand Flume of WL Delft Hydraulics. The length and width of the flume's measurement section were 50 m and 1.0 m, respectively. A mixture composed of three well-sorted grain size fractions was used. During the experiments uniform conditions were maintained and the transported sediment was recirculated. As a result net aggradation or degradation did not occur. The sediment transport consisted solely of bed load transport [*Blom et al.*, 2003].

Experiment B2 started from the final stage of experiment B1. The initial bed of B2 consisted of a coarse bed layer on top of a substrate composed of only the fine size fraction. Small barchan-type bed forms were present on top of this coarse top layer (Figure 1). Right after the start of the experiment, the discharge was increased and the coarse layer was entrained. After this, the underlying fine sediment became available to the transport process and the bed form height quickly increased. The volume fraction of the fine size fraction in the transported material gradually increased, whereas the proportion of the medium and coarse fractions in the transported material slowly decreased, since they were gradually worked down to lower bed elevations. The coarse material in the lower parts of the bed forms did
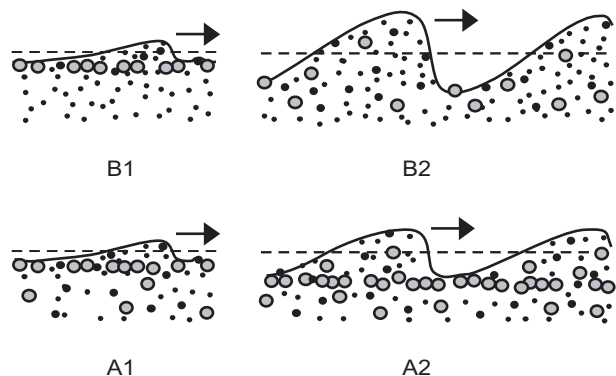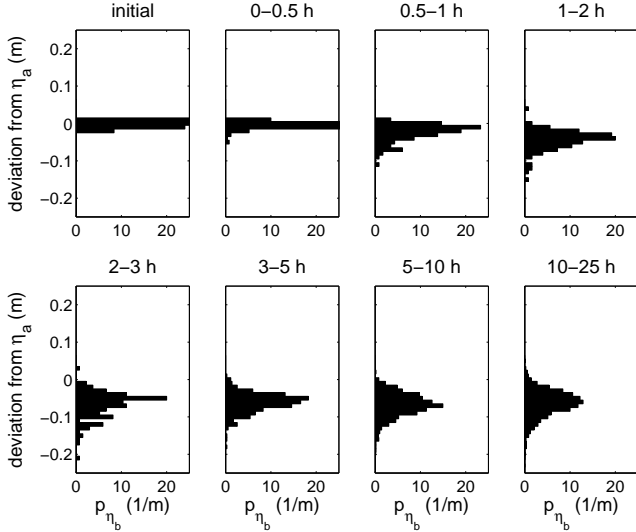

Figure 1. Interpretation of equilibrium stages of experiments B2 and A2 [*Blom et al.*, 2003].

Figure 2. Times (in flow hours) of the core sampling sessions in the experiments with the tri-modal mixture [*Blom et al.*, 2003].

Figure 3. Measured time evolution of the PDF of relative trough elevations, $\tilde{p}_{\eta_b}$, for experiment B2.

not constitute a distinct coarse bed layer over which the bed forms migrated, but participated in the transport process. The vertical sorting profile seemed to be primarily determined by grain size-selective deposition down the avalanche lee face.

Experiment A2 started from the final stage of experiment A1. The initial bed of A2 consisted of a coarse bed layer on top of a substrate composed of a mixture of equal proportions of the three size fractions. Small barchan-type bed forms were present on top of this coarse top layer (Figure 1). Right after the start of the experiment, the discharge was increased to the same rate as in B2. The bed form height increased and the volume fraction of the coarse fraction in the transported material quickly increased. The lower elevations of the active bed showed a clear coarsening compared with the upper ones. The vertical sorting profile seemed to be determined by the grain size-selective deposition down the avalanche lee face, as well as by the winnowing of fines from the trough surface and subsurface, and partial transport.

Table 1 lists the main parameters which were averaged over the period in which all variables varied around stable values. The symbols denote the water depth (h), the average flow velocity (u), the Froude number (Fr), the energy slope (i_E), the Chézy roughness coefficient (C), the hydraulic radius (R), and the bed shear stress (τ), the average bed form length (λ_a), the average bed form height (Δ_a), the average bed form migration speed (c), the volume of total load transport per unit width and time (q_a), and the volume fraction contents of the fine, medium, and coarse size fractions in the total load transport (F_{a1}, F_{a2}, and F_{a3}, respectively) averaged over the equilibrium periods. The Chézy roughness coefficient, the hydraulic radius, and the bed shear stress

were corrected for side wall roughness, using the method of *Vanoni and Brooks* [1957].

Vertical sorting profiles were measured using a core sampling box [*Blom et al.*, 2003]. The core samples were cut into thin layers which were sieved separately. In addition to the initial stage and the equilibrium stage (E-stage), samples were also taken once before equilibrium was reached (the non-equilibrium N-stage) in order to study the time evolution of the sorting profile (see Figure 2). In each sampling session, about 15 core samples were taken.

For a more extensive description of the experiments, we refer to *Blom et al.* [2003].

3. The morphodynamic model system

Figure 1 in *Blom et al.* [2007] shows an overview of the various sub-models in a morphodynamic model system in the case the sorting evolution model is applied.

In the experiments, no net degradation or degradation occurred. In other words, the mean bed level remained steady and sediment fluxes through net aggradation or degradation (type III) did not occur. Sediment fluxes through unsteady PDF of trough elevations (type I) and through dune migration (type II) are included as proposed by *Blom et al.* [2007].
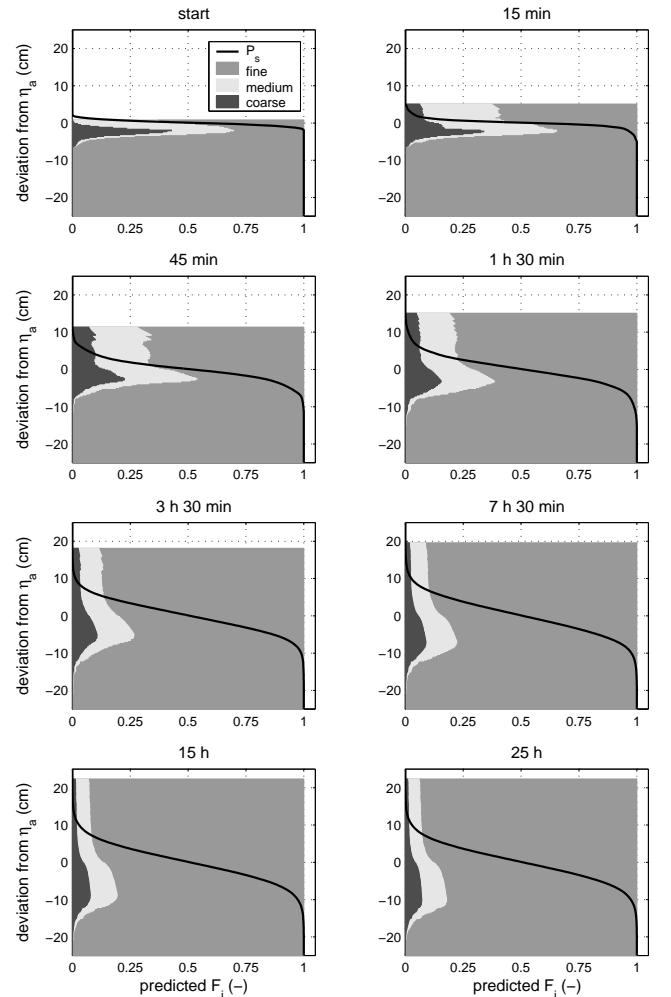
Figure 4. The computed time evolution of the sorting profile, $\bar{F}_i$, for experiment B2. The solid line represents the probability distribution of bed surface elevations, $\bar{P}_s$, in the corresponding phase of the experiment.

Table 1. Experimental parameters, averaged over the equilibrium period [*Blom et al.*, 2003].

exp.	h	u	Fr	i_E	C	R	τ	λ_a	Δ_a	c	q_a	F_{a1}	F_{a2}	F_{a3}
	m	m/s	-	10^{-3}	$m^{1/2}$/s	m	N/m²	m	cm	m/h	m²/s	-	-	-
A2	0.320	0.83	0.47	1.8	38	0.271	4.6	1.38	4.9	8.8	4.310^{-5}	0.38	0.38	0.24
B2	0.389	0.69	0.35	2.2	25	0.351	7.4	1.79	12.2	3.7	4.510^{-5}	0.90	0.05	0.05

In the present case-study, measured values for the PDF of relative trough elevations have been used. A model predicting the time evolution of the PDF of relative trough elevations is therefore not required.

As the bed roughness and the bed load transport were measured during the experiments, models predicting the mean bed surface composition and the flow are not required. The sediment transport consisted solely of bed load transport [*Blom et al.*, 2003]. Hence, the method proposed by *Blom et al.* [2007] for including suspended load transport has not been tested.

4. Unsteady PDF of trough elevations

We account for the time evolution of the PDF of relative trough elevations by following the procedure described in section 4 of the accompanying paper. This means that at the moments the PDF of relative trough elevations is assumed to change in time, sediment is artificially rearranged over bed elevations. Figure 3 shows the measured time evolution of the PDF of relative trough elevations, $\tilde{p}_{\eta_b}$, for experiment B2. We can see that the greatest changes in the PDF of relative trough elevations occur within 0 to 2 flow hours. After that, only small changes occur.

The time series of the PDF of relative trough elevations is used as input to the sorting evolution model. Note that trough elevations above the mean bed level have been neglected. The PDF of relative trough elevations is imposed to change in time at the transitions between the periods shown in Figure 3.

5. Time evolution of vertical sorting

We apply equation (12) in the accompanying paper [*Blom et al.*, 2007] to describe the time evolution of sorting in a situation without net aggradation or degradation. Note that the ratio between the average bed form length, λ_a, the average bed form height, Δ_a, and the total bed load transport rate, $\bar{q}_a$, are assumed to be steady during the experiments. Their values have been set equal to their equilibrium values, which are given in Tables 2 and 3 in *Blom et al.* [2003]. The angle of repose of the lee faces is assumed to be equal to 30°. The initial sorting profiles of experiments B2 and A2 equal the measured sorting profiles (final stage of experiments B1 and A1, respectively).

Figure 4 shows the computed (and measured) time evolution of the vertical sorting profile, as well as the probability distribution of bed surface elevations, $\bar{P}_s$, at the specific time. Equations (23) and (24) in the accompanying paper show how $\bar{P}_s$ is determined from the given time evolution of the PDF of relative trough elevations. Figure 4 shows how the computed sorting pattern of experiment B2 gradually develops towards its equilibrium profile and that the range of active bed elevations over which the sorting takes place increases. The coarse particles settle primarily to the lower lee face elevations and the finer particles to the upper lee face elevations. Figure 4 illustrates that at the lower elevations of the active part of the bed the grain size distribution adapts more slowly than at the upper ones.

Note that the inflection point of the vertical sorting profile is always located at the mean bed level. This is due to the way of modeling grain size-selective deposition down a lee face in combination with the irregularity of bed forms. Individual stoss and lee faces are assumed to be anti-symmetric

around the mean bed level (see Figure 6 in *Blom et al.* [2006]).

In Figure 5, the computed sorting profiles are compared to the measured ones, for the non-equilibrium stage and the equilibrium stage of experiment B2, stages B2N and B2E, respectively (Figure 2). The measured sorting profile of phase B2E shows a top layer coarser than the material underneath. This is due to (1) the formation of a thin mobile armour layer over the stoss face and (2) deposition of sediment that was being transported until the flow was turned off. This phenomenon has also been addressed in the calibration of the equilibrium sorting model by *Blom et al.* [2006]. The computed sorting profiles do not show such a coarse top layer, since in the sorting evolution model it is assumed that the composition of the net entrainment flux on the stoss face has the same composition as the bed material at that elevation.

The computed sorting profile for the non-equilibrium stage (B2N) shows reasonable agreement with the data. The sorting trend is somewhat too strong, but the computed volume fraction contents of the size fractions have the right order of magnitude. The computed sorting profile for the equilibrium stage B2E agrees well with the measured one, considering the large variation in the sorting profiles from different core samples.

Note that the range of bed elevations covered by the core samples is small compared to the range of elevations covered by the computations (Figure 5). The measured range
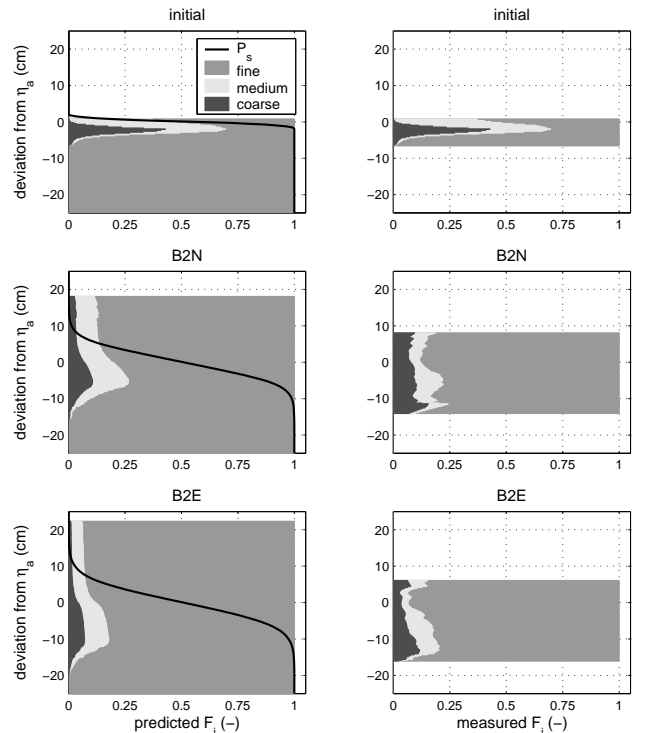
Figure 5. Comparison of the measured and computed sorting profiles, $\bar{F}_i$, for the non-equilibrium stage and the equilibrium stage of experiment B2.

of bed elevations shows the range covered by the core samples, while the computed range is the range of *active* bed elevations. The latter is based on the PDF of measured trough elevations, as well as on the assumption that each bed form crest is located at the same vertical distance from the mean bed level as its trough. In reality, however, the deepest bed form troughs are usually not accompanied by the highest crests [*Leclair and Blom*, 2005]. This causes the computed range of active bed elevations to be larger than the measured one. Yet, since the probability density of these upper elevations being exposed to the flow, $\bar{p}_e$, is very small, these elevations have negligible influence on, for instance, the composition of the sediment transported over the crests. More important to the sorting evolution calculations than these upper elevations are the lower elevations of the active bed. Unfortunately, these lower elevations are not entirely covered by the core samples.
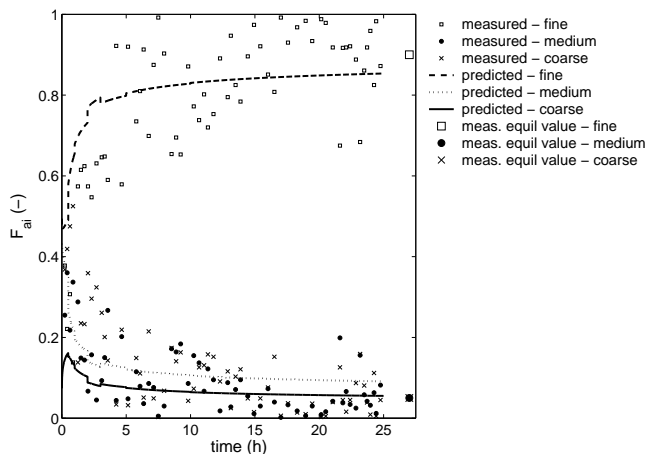
Figure 6 shows the measured and computed time evolution of the average composition of the bed load transport for experiment B2. The agreement between the measured and computed time evolution of the average transport composition is reasonably good, which implies that the physical mechanisms are simulated rather well by the model. The computed values are close to the measured composition of the sediment transport averaged over the equilibrium period. Note that the 'creases' in the computed composition are not due to numerical problems, but to the imposed transitions in the time evolution of the PDF of relative trough elevations (see Figure 3).

Since conditions were uniform in the experiments, the amount of sediment integrated over all elevations of the active bed, $\bar{C}_{tot}$,

$$\bar{C}_{tot} = \int_{\eta_{mn}}^{\eta_{mx}} \bar{C}_i(z)\, dz = \int_{\eta_{mn}}^{\eta_{mx}} c_b \bar{P}_s(z) \bar{F}_i(z)\, dz \qquad (1)$$

must be constant. Here η_{mn} and η_{mx} denote the limits of the active bed in the stage in which the active bed covers the widest range of bed elevations. Also, the volume fraction content of each grain size fraction in the bed, $\bar{\bar{F}}_i$, which is given by equation (63) in *Blom et al.* [2006], must be steady. This is confirmed.

Figure 7 considers flume experiment A2. The initial sorting profile of the experiment was the final stage of experiment A1 (stage A1E), in which small bed forms migrated
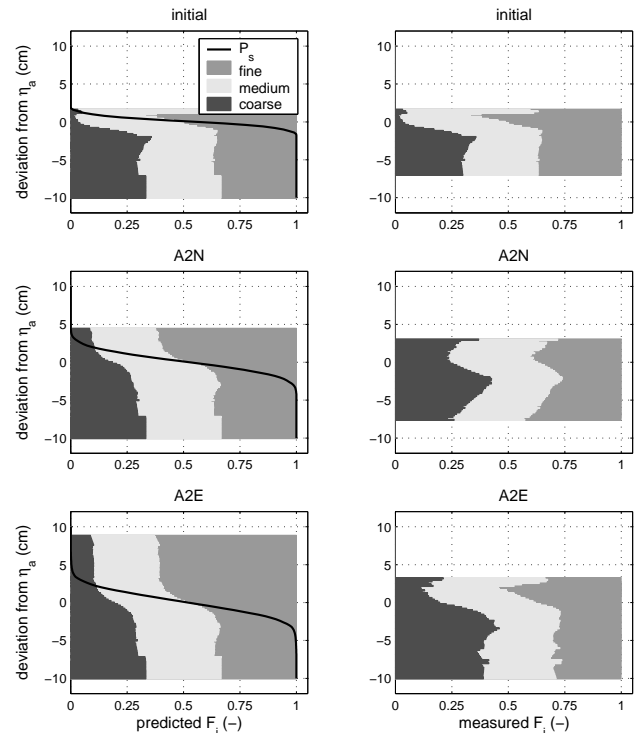
over a coarse bed layer. During the experiment, the downward coarsening trend remains, but covers an increasing range of bed elevations. Comparing the computed sorting profiles with the measured ones (Figure 7), we can see that the formation of the coarse layer is not adequately described by the model. The disagreement between the computed and measured sorting profiles is larger for A2 than for B2, which appears to be due to the model's inadequate description of the formation of a coarse bed layer. In the sorting evolution model, the dominant sorting mechanism is the grain size-selective deposition down a bed form lee face. The present version of the model does not account for the mechanisms of (1) the winnowing of fines from the trough surface and subsurface and (2) the settling of immobile coarse grains, whereas these mechanisms play a significant role in the formation of a coarse bed layer.

Figure 8 illustrates that the computed time evolution of the average composition of the sediment transport lies within the scatter of the measured data. The computed values are fairly close to the measured composition of the sediment transport averaged over the equilibrium period.

6. Towards equilibrium

For both experiments B2 and A2, calculations have been continued until 500 flow hours. Figure 9 shows the computed time evolution of the bed load transport composition. Note the log-scale on the horizontal axis. The figure illustrates that, at the end of the experiments (B2 at 25 flow hours, A2 at 18 flow hours), the computed bed load transport composition is already close to its equilibrium composition. This also applies to the sorting profiles (see Figure 10). Between the end of the experiment and 500 flow hours, mainly the very

Figure 6. Measured and computed time evolution of the volume fraction content of size fractions in the bed load transport, $\bar{F}_{ai}$, for experiment B2. Note that the large markers on the right-hand side of the plot represent the measured composition of the bed load transport averaged over the equilibrium period.

Figure 7. Comparison of the measured and computed sorting profiles, $\bar{F}_i$, for the non-equilibrium stage and the equilibrium stage of experiment A2.

low elevations of the active bed continue adapting towards their equilibrium compositions. This adaptation influences the composition of the bed load transport only slightly (Figure 9).

7. Comparison with the Hirano and Ribberink sediment continuity models

Blom and Parker [2004] have presented an overview of existing sediment continuity models. It was explained that the Hirano active layer model suffers from a number of shortcomings. The most important one is the neglect of vertical sediment fluxes other than through net aggradation or degradation. The assumption that the bed material interacting with the flow can be represented by a distinct surface layer, as proposed by *Hirano* [1971], seems to be too limited to adequately account for sorting processes acting in the river bed. *Ribberink* [1987] recognized the influence of relatively deep bed elevations interacting with the flow and being subject to entrainment and deposition less frequently than higher ones. In order to account for the exchange of sediment through occasional deep bed form troughs, *Ribberink* introduced an additional bed layer below the active layer, i.e. the exchange layer, together with a term describing the sediment exchange between the active layer and the exchange layer. The exchange layer represents the elevations exposed to the flow only occasionally, whence the adaptation time scale of its composition is much larger than the one

of the active layer. Still, the introduction of the exchange layer does not completely solve another shortcoming of existing bed layer models, viz. that in certain situations the set of equations becomes elliptic in parts of the space-time domain [*Ribberink*, 1987]. This means that solving the set of equations would require future time-boundaries, which is physically unrealistic. A limitation of the present version of the Ribberink two-layer model is that the formulation for the sediment exchange between the active layer and the exchange layer is only applicable to mixtures composed of two grain size fractions.

The present section presents a quantitative comparison of the predictive abilities of the Hirano active layer model, the Ribberink two-layer model, and the new sorting evolution model. The models are applied to the flume experiments B2 and A2. Since the experiments are characterized by conditions without net aggradation or degradation, we can reduce the equations of the Hirano active layer model and the Ribberink two-layer model.

Sediment continuity of the Hirano active layer now yields

$$c_b \frac{\partial F_{mi}\,\delta}{\partial t} + c_b\,F_{Ii}\,\frac{\partial \eta_I}{\partial t} = -\frac{\partial F_{ai}\,q_a}{\partial x} = 0 \qquad (2)$$

where δ denotes the thickness of the active layer, η_I the elevation of the interface between the active layer and the substrate, F_{mi} the volume fraction content of size fraction i in the active layer, F_{Ii} the volume fraction content of size fraction i at the interface between the active layer and the substrate, F_{ai} the volume fraction content of size fraction i in the transported material, and q_a the volume of sediment transport per unit width and time. All parameters are averaged over some horizontal distance, e.g., a large number of bed forms. For simplicity, the width is assumed to be uniform and the sediment concentration in the bed ($c_b = 1-\lambda_p$) is assumed to be steady and uniform. The volume fraction content of size fraction i at the interface between the active layer and the exchange layer, F_{Ii} is given by

$$F_{Ii} = \begin{cases} F_{mi} & \text{rising interface} \\ F_{oi} & \text{lowering interface} \end{cases} \qquad (3)$$

where F_{oi} denotes the volume fraction content of size fraction i in the substrate. The second term in (2) cannot be neglected, since we include the effects of changes in time of
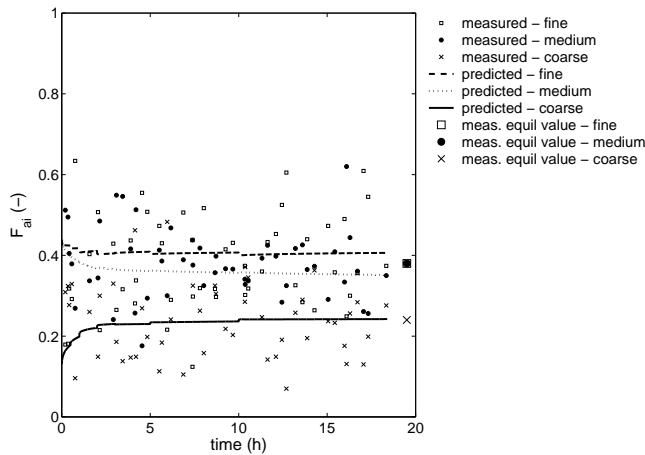
Figure 8. Measured and computed time evolution of the volume fraction content of size fractions in the bed load transport, $\bar{F}_{ai}$, for experiment A2. Note that the large markers on the right-hand side of the plot represent the measured composition of the bed load transport averaged over the equilibrium period.
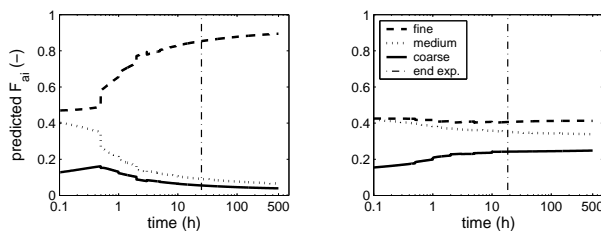
Figure 9. The computed composition of the bed load transport until 500 flow hours, for (a) experiment B2 and (b) experiment A2. Note the log-scale on the x-axis.
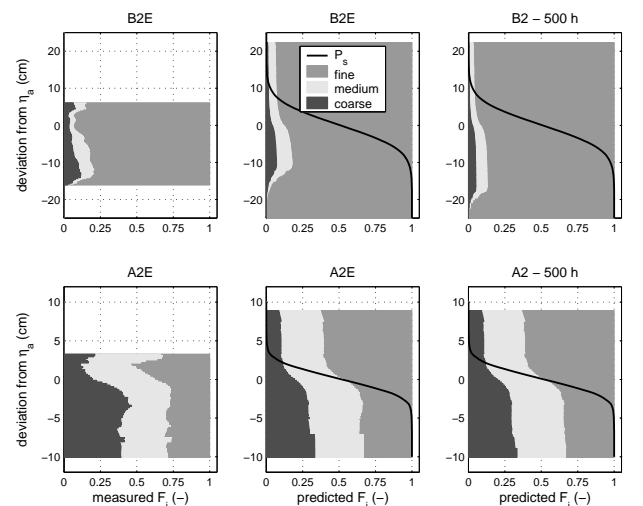
Figure 10. The measured sorting profile at the end of the experiment, the computed sorting profile at the end of the experiment, and the computed sorting profile after 500 flow hours, for experiments B2 and A2.

the bed form height and thus of the active layer thickness. This implies that also the level of the interface, η_I, varies in time:

$$\eta_I(t) = \bar{\eta}_a - \delta(t) \qquad (4)$$

For this reason, the original terms 'aggradation' and 'degradation' in the expression for F_{Ii} have been rephrased to 'rising interface' and 'lowering interface', respectively.

In the computations presented in this section, we divide the substrate into multiple layers, as was proposed by *Sloff et al.* [2001]. In this way, the model system registers and remembers the composition of previously deposited sediment, which is important in situations when degradation follows aggradation. In the present case, in which no net aggradation or degradation occurs, dividing the bed into multiple layers is important for another reason. The initial average bed form height, and thus the thickness of the active layer, is very small. This is due to the small dunes present at the initial stage of the experiment. Would we not impose the (large) variation of the initial sorting profile over depth, computations would yield worse results.

Using equation (2), we can solve for the time evolution of the composition of the active layer, F_{mi}, from the given time evolution of the active layer thickness, δ. Because of the registration over a large number of bed elevations, we not only solve for the time evolution of the composition of the active layer, but for the time evolution of the complete sorting profile, $\bar{F}_i$.

For cases without net aggradation or degradation, the fundamental equations , sediment continuity of the active layer and the exchange layer in the Ribberink two-layer model then yield

$$\frac{\partial F_{mi}\delta}{\partial t} + F_{Ii}\frac{\partial \eta_I}{\partial t} = \psi_i - \frac{\partial F_{ai}q_a}{\partial x} = \psi_i \qquad (5)$$

$$\frac{\partial F_{ei}\delta_e}{\partial t} + F_{IIi}\frac{\partial \eta_{II}}{\partial t} - F_{Ii}\frac{\partial \eta_I}{\partial t} = -\psi_i \qquad (6)$$

where

$$F_{Ii} = \begin{cases} F_{mi} & \text{rising interface I} \\ F_{ei} & \text{lowering interface I} \end{cases}$$

$$F_{IIi} = \begin{cases} F_{ei} & \text{rising interface II} \\ F_{oi} & \text{lowering interface II} \end{cases}$$

where δ_e denotes the thickness of the exchange layer, F_{ei} denotes the volume fraction content of size fraction i in the exchange layer, F_{Ii} denotes the volume fraction content of size fraction i at the interface between the active layer and the exchange layer, and F_{IIi} denotes the volume fraction content of size fraction i at the interface between the exchange layer and the substrate. The sediment exchange term, ψ_i, is given by

$$\psi_i = E_{ti} - D_{ti} = \gamma_t \frac{q_a}{\lambda_a}(F_{ei} - F_{miD})$$

Using these equations, we can solve for the time evolution of both the composition of the active layer, F_{mi}, and the composition of the exchange layer, F_{ei}, from the given time evolution of both the active layer thickness, δ, and the exchange layer thickness, δ_e. Again, as we register the bed composition over a larger range of bed elevations, we can compute the time evolution of the complete sorting profile, $\bar{F}_i$.

Following *Ribberink* [1987], the active layer thickness and the exchange layer thickness are computed from the average bed form height:

$$\delta(t) = 0.5\,\Delta_a(t)$$

$$\delta_e(t) = 1.22\,\delta(t)$$

Herein, the time evolution of the average bed form height is accounted for. Transitions in the average bed form height occur at the same points in time as the PDF of trough elevations was assumed to change in time (Figure 3).

Since the sediment mixtures used in experiments B2 and A2 were not bi-modal but tri-modal, the description of sediment exchange between the active layer and the exchange layer in the Ribberink two-layer model first needs to be extended. *Ribberink* [1987] supposed the sediment deposited from the active layer into the exchange layer to be somewhat coarser than the average composition of the active layer, because of the downward coarsening trend within the bed forms. For a bi-modal mixture, *Ribberink* found that the volume fraction content of the *finest* fraction deposited from the active layer into the exchange layer is about 70% of that in the active layer:

$$F_{m1D} = 0.7\,F_{m1} \qquad (7)$$

For a mixture of two size fractions, the volume fraction content of the coarse size fraction deposited from the active layer into the exchange layer now logically equals

$$F_{m2D} = 1 - F_{m1D} \qquad (8)$$

The subscripts 1 and 2 indicate the fine and coarse size fractions, respectively. Note that (10) and (8) only apply to *bi-modal mixtures*. Now, for a tri-modal mixture and following (10) for the finest size fraction, we adapt the formulation for sediment exchange to

$$F_{m1D} = 0.7\,F_{m1} \qquad (9)$$

$$F_{m2D} = F_{m2} \qquad (10)$$

$$F_{m3D} = 1 - F_{m1D} - F_{m2D} \qquad (11)$$

Note that these equations comprise only an ad-hoc formulation for the sediment deposited from the active layer into the exchange layer. The formulation has not been calibrated.

For experiments B2 and A2, the imposed initial sorting profile is identical to the measured equilibrium sorting profile of experiments A1 and B1, respectively. The time evolution of the sorting profile as computed by the Hirano active layer model, the Ribberink two-layer model, and the sorting evolution model is now compared to measured data from the experiments. For experiment B2, the results of these computations are presented in Figure 11.

The left column of plots in Figure 11 shows the measured vertical sorting profiles in experiment B2: (a) its initial B1E stage, (b) the non-equilibrium B2N stage, and (c) the equilibrium B2E stage. We can see how the medium and the coarse size fraction, initially located in the upper parts of the bed, become redistributed over a large range of bed elevations.

The second column of plots in Figure 11 shows the time evolution of sorting in experiment B2 as computed by the Hirano active layer model. In the initial phase, the active layer thickness is very small (look closely to see the very thin homogeneous active layer in the upper plot of the second column), which concurs with the small dunes present in the initial stage of the experiment. After the start of experiment B2, the imposed average bed form height and so the active layer thickness increase quickly. Figure 11 shows that the Hirano active layer model is not able to reproduce the time evolution of the sorting profile in experiment B2. This is not surprising considering the neglect of vertical sorting fluxes in the model.

The third column of plots in Figure 11 shows the time evolution of sorting in experiment B2 as computed by the Ribberink two-layer model. In the initial phase, the active
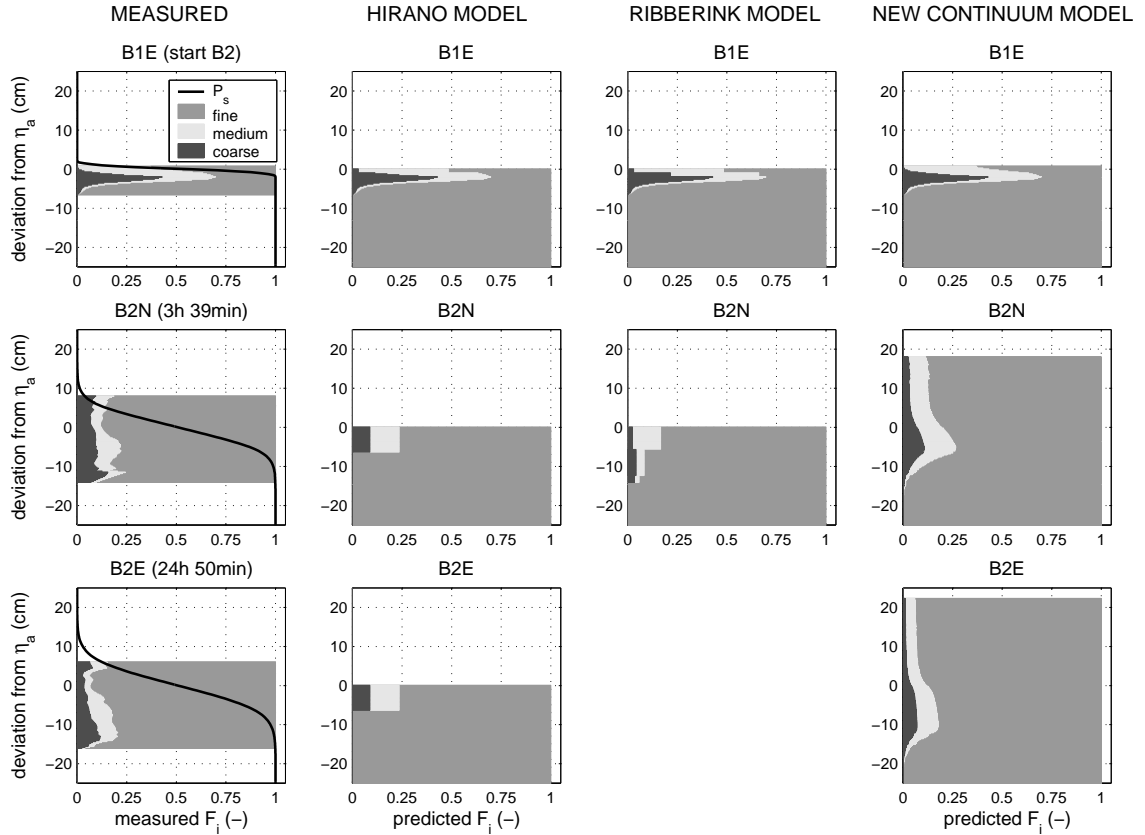
Figure 11. The measured time evolution of vertical sorting in experiment B2, and the vertical sorting as computed by the Hirano active layer model, the Ribberink two-layer model, and the sorting evolution model.

layer thickness and exchange layer thickness are very small, due to the small dunes present in the initial stage of the experiment. With respect to the range of elevations of the active bed, the model shows better results than the Hirano model. However, for the conditions of experiment B2 the two-layer model appears to behave problematically: it does not guarantee continuity of grain size fractions. This can be understood from the following. The present formulation for the composition of the deposition flux from the active layer to the exchange layer, F_{miD}, given by equation (9)-(11), causes the small amount of the coarse size fraction in the active layer to be deposited to the exchange layer. This is due to the fact that the proportion of the fine size fraction in the deposition flux from the active layer to the exchange layer is imposed to be equal to 70% of the proportion of this size fraction in the active layer, which implies that the remaining 30% in this deposition flux is composed of the medium and coarse size fractions. Since experiment B2 is characterized by a large amount of the finest size fraction, this procedure causes the coarse fraction in the active layer to become exhausted. Even when the active layer no longer consists of coarse sediment, equation (11) still imposes that some percentage of the deposition flux from the active layer to the exchange layer is composed of the coarse fraction. This is physically impossible and 'creates' sediment of the coarse fraction. Although the formulation for the sediment exchange of a mixture of three grain size fractions is only an ad-hoc formulation, the problem can occur for a mixture of two grain size fractions, as well.

The fourth column of plots in Figure 11 shows the time evolution of sorting in experiment B2 as computed by the sorting evolution model. These results have been discussed in section 5. Reference is made to Figure 5 and the accompanying text.

Figure 12 shows the results of the computations for experiment A2. Like for experiment B2, the range of elevations

covered by the Hirano active layer is much smaller than the measured range of elevations exposed to the flow. Again, the Ribberink model shows much better results in predicting the range of elevations of the active bed. The Ribberink two-layer model performs in a better way than for B2, since now the coarse size fraction in the active layer does not become exhausted.

8. Time scales

For experiments B2 and A2, Figure 13 shows the time scale of the adaptation of sorting, $T_f(z)$, according to equation (40) in the accompanying paper [*Blom et al.*, 2007], together with the time scale of dune migration, T_c, which is defined as the time required for a bed form to cover the average bed form length, $\bar{\lambda}$:

$$T_c = \bar{\lambda}/c \qquad (12)$$

In the lower parts of the active bed, the time scale of sorting, $T_f(z)$, appears to be much larger than the time scale of dune migration, whereas in the upper parts the time scale of sorting is smaller than one of dune migration. One of the constraints of the sorting evolution model is, however, that the time scale of migration must be smaller than the time scale of sorting. This constraint arises from the assumption that the sediment deposited at elevation z is immediately mixed with all sediment present at this elevation. This implies that the time evolution of the sorting in the upper parts of the active bed may not be adequately described by the model.

For the Ribberink two-layer model, *Ribberink* [1987] defined a time scale for the adaptation of the composition of

the exchange layer. This exchange layer is located below the active layer and represents the bed elevations exposed only by relatively deep bed form troughs. The time scale of the adaptation of the composition of the exchange layer was defined as

$$T_{f\,Ribb} = \frac{c_b\,\bar{\lambda}}{\gamma_r\,\bar{q}_a}\,\frac{\delta_e}{1 + \alpha_r\,\delta_e/\delta} \tag{13}$$

in which the constant α_r is given by $\alpha_r = d_m/d_{md}$ where d_m denotes the geometric mean grain size of the active layer and d_{md} denotes the geometric mean grain size of the sediment deposited from the active layer to the exchange layer through the variability in trough elevations. Since bed forms mostly show a downward coarsening trend, *Ribberink* [1987] assumes sediment deposited from the active layer to the exchange layer to be coarser than the average composition of the active layer, which implies that α_r is larger than 1. The constant γ_r relates the amount of deposition into the deepest troughs (being equal to the entrainment rate from these deepest troughs) to the bed load transport rate. As recommended by *Ribberink*, we assume $\alpha_r = 1.5$, $\gamma_r = 0.06$, $\delta = 0.5\,\Delta_a$, and $\delta_e = 1.22\,\delta$. The time scale of the adaptation of the exchange layer composition for experiments B2 and A2 is plotted in Figure 13.

According to the present sorting evolution model, for the lower elevations of the active bed, the time scale of sorting is much larger than the time scale of adaptation of the composition of the exchange layer as proposed by *Ribberink* [1987]. This is confirmed by the measured time evolution of the sorting profile in experiments B2 and A2.

9. Discussion and conclusions

The sorting evolution model has been verified by comparing the computed time evolution of both the sorting profile and the bed load transport composition with measured data from experiments B2 and A2. It is important to note that, except for the two constants in the lee sorting function that were verified for equilibrium conditions, no parameters in the sorting evolution model have been calibrated against measurements. The computational results agree reasonably well with the data. Nevertheless, the formation of a coarse bed layer in the lower parts of migrating bed forms is not adequately described by the model. It is emphasized that the sorting evolution model's main sorting mechanism is the grain size-selective deposition over the lee face. The model does not allow for grain size-selective entrainment over the stoss face, as all particles present at a certain elevation of the active bed are assumed to be transported over the bed form crest. Particles present on the stoss face, but too coarse to be transported, are therefore not allowed to settle down as the bed form migrates. Instead, these coarse particles are assumed to be transported over the bed form crest and are then deposited onto the lower elevations of the active bed through the mechanism of grain size-selective deposition down the lee face. Moreover, also the winnowing of fines from the trough surface and subsurface plays a role in the formation of a coarse bed layer and is not included in the model. The mechanisms of winnowing of fines and the settling of immobile coarse particles need to be incorporated in a later version of the model, so as to improve the description of the formation of a coarse bed layer.

Ribberink [1987] explained that the set of equations of the Hirano active layer model may become elliptic in parts of the space-time domain in situations wherein degradation occurs while the substrate is finer than the active layer. A set of equations being elliptic means that, at each point in space and time, the state is determined by the state in all other points. This means that boundary conditions are required at all boundaries of the space-time domain covered by the
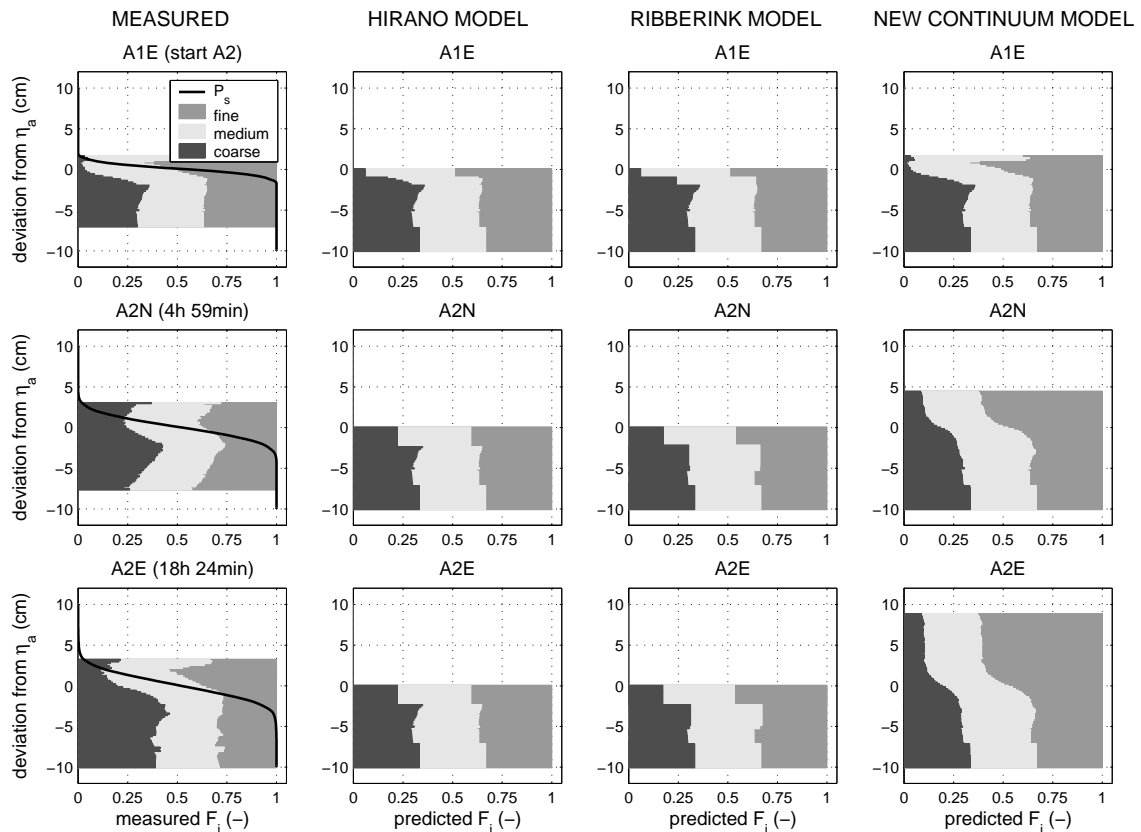
model. Since imposing conditions in the future is physically unrealistic, the active layer model is obviously not able to model the natural processes in those circumstances. It is, however, not straightforward to analyze the set of equations of the new sorting evolution model for possible ellipticity, since its set of equations is much more extensive than the set of equations of the Hirano active layer model. This analysis has therefore not been performed in the present study. Yet, since the ellipticity of the set of equations of the active layer model appears to be related to the instantaneous mixing of sediment within the discrete bed layers [*Ribberink*, 1987], it is believed that the new sorting evolution model will not become elliptic. There has been no evidence that the Armanini diffusion model, which is another depth-continuous model, may become elliptic under certain conditions, which may confirm the idea that a depth-continuous approach at least partly solves the ellipticity problem.

In the present analysis we have used the measured (time evolution of the) PDF of relative trough elevations as input to the sorting calculations. In predictive calculations, we will need to predict the PDF of relative trough elevations, $\tilde{p}_b$, which is required as input to the sorting evolution model. A relatively simple sub-model for the PDF of relative trough elevations is proposed by *Van der Mark et al.* [2005].

It can be concluded that the sorting evolution model shows better results with respect to the computed time evolution of the vertical sorting profile than the active layer model and the two-layer model. Based on the present study, it seems to be possible to improve the formulation for the sediment exchange between the *Hirano* [1971] active layer and the exchange layer in the *Ribberink* [1987] two-layer model. The author would suggest relating the volume fraction contents of size fractions deposited from the active layer into the exchange layer to both the geometric mean grain size and the arithmetic standard deviation of the active layer material. This would correspond with the formulation for the grain size-selective deposition down the bed form lee face as listed in Appendix B of the accompanying paper. An improved formulation could be derived by integrating the formulations for the vertical sorting fluxes as derived in the present study over certain ranges of bed elevations.

Yet, an important problem of this procedure is that the determination of the elevations of the interfaces (1) between the active layer and the exchange layer, and (2) between the exchange layer and the substrate are arbitrary. In other words, no matter how the active layer thickness and the exchange layer thickness are defined, these definitions will always be ambiguous. From a physical point of view, there is no support for the definition of discrete bed layers, as can be seen from the measured sorting profiles in Figures 11 and 12. For instance, the variation of the bed composition over bed elevations is continuous and does not show sudden transitions. It is therefore recommended to eventually leave the concept of discrete bed layers and step over to depth-continuous models. However, from an engineering point of view, it is useful to improve the formulation for the sediment exchange between the active layer and the exchange layer in the Ribberink two-layer model.

Figure 12. The measured time evolution of vertical sorting in experiment A2, and the vertical sorting as computed by the Hirano active layer model, the Ribberink two-layer model, and the sorting evolution model.

References

Blom, A., and G. Parker (2004), Vertical sorting and the morphodynamics of bedform-dominated rivers: A modeling framework, *J. Geophys. Res.*, *109*, F02007, doi:10.1029/2003JF000069.

Blom, A., J. S. Ribberink, and H. J. de Vriend (2003), Vertical sorting in bed forms: Flume experiments with a natural and a trimodal sediment mixture, *Water Resour. Res.*, *39*(2), 1025, doi:10.1029/2001WR001088.

Blom, A., G. Parker, J. S. Ribberink, and H. J. de Vriend (2006), Vertical sorting and the morphodynamics of bed-form-dominated rivers: An equilibrium sorting model, *J. Geophys. Res.*, *111*, F01006, doi:10.1029/2004JF000175.

Blom, A., J. S. Ribberink, and G. Parker (2007), Vertical sorting and the morphodynamics of bedform-dominated rivers: A sorting evolution model. 1. Derivation, *submitted to J. Geophys. Res.*

Hirano, M. (1971), River bed degradation with armouring, *Transactions Jap. Soc. Civ. Eng.*, *3*(2), 194–195.

Leclair, S. F., and A. Blom (2005), A qualitative analysis of the distribution of bed-surface elevation and the characteristics of associated deposits for subaqueous dunes, in *Fluvial Sedimentology VII, Spec. Publs. Int. Ass. Sediment.*, edited by M. D. Blum, S. B. Marriott, and S. F. Leclair, pp. 121–134.

Parker, G., C. Paola, and S. Leclair (2000), Probabilistic Exner sediment continuity equation for mixtures with no active layer, *J. Hydraul. Eng.*, *126*(11), 818–826.

Ribberink, J. S. (1987), Mathematical modelling of one-dimensional morphological changes in rivers with non-uniform sediment, Ph.D. thesis, Delft University of Technology, the Netherlands.

Sloff, C. J., H. R. A. Jagers, Y. Kitamura, and P. Kitamura (2001), 2D Morphodynamic modelling with graded sediment, in *Proc. 2nd IAHR Symposium on River, Coastal and Estuarine Morphodynamics*, edited by S. Ikeda, pp. 535–544, Obihiro, Japan.

Van der Mark, C. F., A. Blom, S. J. M. H. Hulscher, S. F. Leclair, and D. Mohrig (2005), On modeling the variability of bedform dimensions, in *Proc. IAHR Symposium on River, Coastal and Estuarine Morphodynamics*, edited by G. Parker and M. H. Garcia, pp. 831–841, Taylor & Francis Group, London, Urbana, Illinois, USA.

Vanoni, V. A., and N. H. Brooks (1957), Laboratory studies of the roughness and suspended load of alluvial streams, *Technical Report E-68*, Sedimentation Laboratory, California Institute of Technology, Pasadena, USA.

A. Blom, University of Twente, Civil Engineering, P.O. Box 217, 7500 AE Enschede, Netherlands. (a.blom@utwente.nl)

J. S. Ribberink, University of Twente, Civil Engineering, P.O. Box 217, 7500 AE Enschede, Netherlands. (j.s.ribberink@utwente.nl)

G. Parker, Department of Civil and Environmental Engineering and Department of Geology, University of Illinois at Urbana-

Champaign, Urbana IL 61801, USA. (parkerg@uiuc.edu)
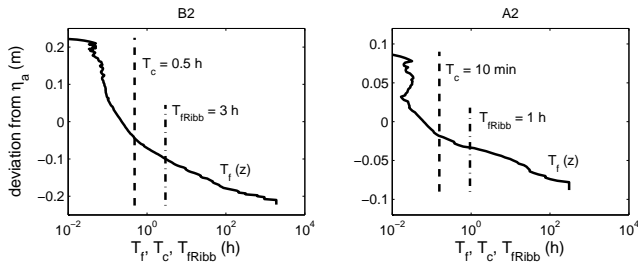
Figure 13. The time scale of the adaptation of sorting, $T_f(z)$, according to equation (36) in *Blom et al.* [2007], the time scale of dune migration, T_c, according to (12), and the time scale of the exchange layer composition according to (13), for experiments B2 and A2. Note the log-scale on the x-axis.